I&EC research
Industrial & Engineering Chemistry Research

Article

pubs.acs.org/IECR

Cerium Oxide Coating of Titanium Dioxide Pigment to Decrease Its Photocatalytic Activity

Han Gao, Bing Qiao, Ting-Jie Wang,* Dezheng Wang, and Yong Jin

Department of Chemical Engineering, Tsinghua University, Beijing, 100084, China

ABSTRACT: The use of cerium oxide coating of titanium dioxide pigments to decrease photocatalytic activity was studied. A large decrease in the photocatalytic activity of titanium dioxide particles coated with cerium oxide was obtained even with a tiny coating amount of 0.2 wt %, and these particles were more stable than those with the conventional 2.0 wt % film coating of silicon dioxide or 1.5 wt % aluminum oxide. The combination film coatings of cerium oxide and silicon or aluminum oxide showed smaller decreases in photocatalytic activity. Both Ce(III) and Ce(IV) oxide coatings gave highly decreased photocatalytic activity, even when the cerium oxide coating did not completely cover the surface. It was inferred that the efficient decrease of photocatalytic activity was because the unpaired electrons in the 4f orbital of cerium enabled the coating film to capture electrons and holes that were produced when titanium dioxide was exposed to ultraviolet irradiation.

1. INTRODUCTION

Titanium dioxide (TiO_2), which is chemically inert and nontoxic, is the best white pigment due to its excellent optical properties. It is widely used in the paint, plastic, and paper industries. However, TiO_2 particles have photocatalytic activity. Organic substrates in the paint layer are easily oxidized and decomposed by the photocatalytic activity of TiO_2 particles, which result in the degradation of the paint film.[1−3]

The electron−hole mechanism for photocatalytic reactions on the TiO_2 surface is widely accepted. This has the steps of the separation of the electron and hole, formation of free radicals, and oxidation of the free radicals.[4,5] The reaction is started when light irradiation causes an electron in the valence band of TiO_2 to be excited into the conduction band.[6]

$$h\nu \rightarrow e^- + h^+ \quad (1)$$

The electron in the conduction band and the hole formed in the valence band diffuse to the surface of TiO_2 where they react with H_2O, O_2, and OH^-[7,8] to produce free radicals with strong oxidizing abilities. The reactions of the hole are

$$h^+ + H_2O \rightarrow \bullet OH + H^+ \quad (2)$$

$$h^+ + OH^- \rightarrow \bullet OH \quad (3)$$

The reactions of the electron are complicated. One theory is that an electron reacts with O_2 and H_2O to produce free radicals:[5,6]

$$e^- + O_2 \rightarrow \bullet O_2^- \quad (4)$$

$$\bullet O_2^- + H_2O \rightarrow \bullet OOH + OH^- \quad (5)$$

$$e^- + \bullet OOH + H_2O \rightarrow H_2O_2 + OH^- \quad (6)$$

$$2\bullet OOH \rightarrow O_2 + H_2O_2 \quad (7)$$

$$e^- + H_2O_2 \rightarrow OH^- + \bullet OH \quad (8)$$

Another theory is that the reaction proceeds by the steps of formation of Ti^{3+}, formation of O_2^-, and formation of free radicals.[9] For this, the electron is first captured by Ti^{4+},[5,10,11]

$$Ti^{4+} + e^- \rightarrow Ti^{3+} \quad (9)$$

Ti^{3+} defect formation can occur both inside and on the surface of TiO_2.[12−14] The formation of Ti^{3+} on the surface would increase the photocatalytic activity as it prevents the recombination of an electron with a hole, and Ti^{3+} can also react with O_2 to form O_2^-, which is also reactive.[15−17] Suriye[18] reported an increase in the photocatalytic activity of TiO_2 with an increase in the concentration of Ti^{3+} on the surface of TiO_2 particles. However, inside the TiO_2 particle, Ti^{3+} would act as an electron−hole trap to decrease the photocatalytic activity of TiO_2.

There are two different Ti^{3+} sites: (a) five-coordinate Ti^{3+} and (b) oxygen vacancy Ti^{3+}. The formation mechanisms of O_2^- are different on these.[15,19] The process is shown in Figure 1.

The reactions for the formation of free radicals are as follows:[20,21]

$$O_2^- + 2H^+ \rightarrow 2\bullet OH \quad (10)$$

$$O_2^- + H^+ \rightarrow \bullet O_2H \quad (11)$$

or[22]

$$\bullet O_2H + O_2^- + H^+ \rightarrow O_2 + H_2O_2 \quad (12)$$

$$H_2O_2 + O_2^- \rightarrow \bullet OH + OH^- + O_2 \quad (13)$$

Organic substrates on the TiO_2 particles are easily oxidized by these free radicals.[6] Therefore, to ensure a very low photocatalytic activity of the pigment, it is necessary to prevent the formation of the free radicals by preventing photogenerated electrons and holes from reaching the TiO_2 particle surface.

Many oxides, such as SiO_2, Al_2O_3, and ZrO_2, have been used as coating materials for TiO_2 particles. Film coatings of SiO_2

Received: August 3, 2013
Revised: December 10, 2013
Accepted: December 13, 2013
Published: December 13, 2013

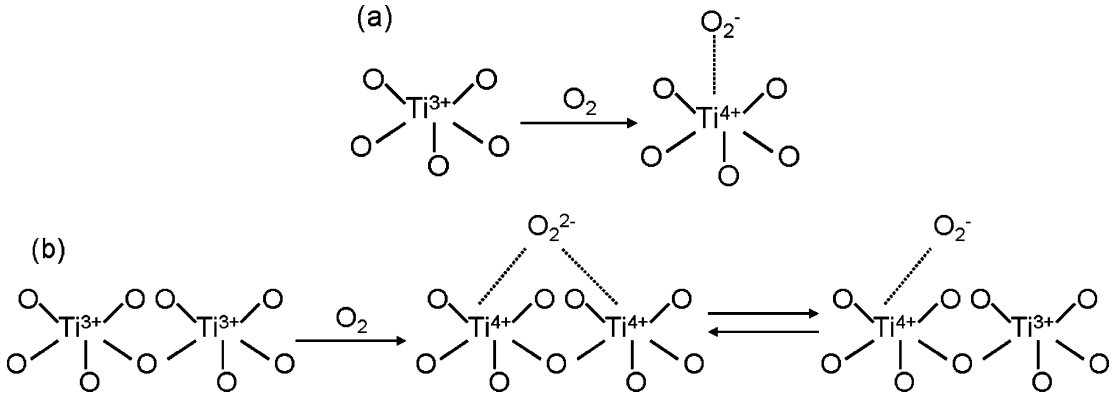

Figure 1. Two different Ti^{3+} sites for O_2^- generation: (a) five-coordinate Ti^{3+}; (b) oxygen vacancy Ti^{3+}.

and Al_2O_3 are widely used in industry for preventing photocatalysis by TiO_2 particles. The coating amount used is generally 3−5 wt %.[23−25] TiO_2 particles coated with other metal oxides, such as those of some transitional metals like zinc, cobalt, and nickel, and lanthanides like that of cerium, were also found to have reduced photocatalytic activity.[26−28] A few literature reports have shown that TiO_2 particles coated with the mixed oxides of cerium, silicon, and aluminum gave larger decreases of photocatalytic activity. European patent 0129960 to Jacobson disclosed that a pigment comprising TiO_2 particles coated with alumina and with cerium cations and sulfate, phosphate, or silicate anions on the particles gave paper laminates that have a high degree of light fastness.[29] US patent 005730796A to Baldwin et al. disclosed that a durable titanium dioxide pigment was obtained from rutile titanium dioxide particles when cerium oxide and dense amorphous silica, and preferably also an outer coating of hydrous alumina, were deposited on it,[30] but the optimized conditions for the cerium oxide coating and the mechanism of photocatalytic activity control were not discussed. It was suggested that cerium oxide mixed with silicon or aluminum oxide on the surface of TiO_2 particles would give a larger decrease in photocatalytic activity.

In this work, the decrease of the photocatalytic activity of TiO_2 particles coated with cerium oxide and combination coatings, with silicon or aluminum oxide in the cerium oxide film, were studied. The photocatalytic activity of the coated TiO_2 particles was evaluated by rhodamine-B degradation under ultraviolet irradiation.

2. EXPERIMENTAL SECTION

2.1. Reagents. Commercial TiO_2 particles (Jiangsu Hongfeng Titanium Company, China) from the sulfate process, in which TiO_2 particles were produced by the hydrolysis of $TiOSO_4$ and a subsequent calcination, were used in the experiments. The TiO_2 particles have the rutile structure and a mean diameter of 300 nm. They were pure without any preliminary treatment. All chemicals used, namely, $Ce(SO_4)_2 \cdot 4H_2O$, $Ce(NO_3)_3 \cdot 6H_2O$, Na_2SiO_3, $Al_2(SO_4)_3$, NaOH, H_2SO_4, and rhodamine-B, were analytical reagent (AR) grade.

2.2. Coating Process. Coating experiments were conducted in a flask with the temperature and pH monitored online with a thermometer and pH meter, respectively. TiO_2 particles at a concentration of 500 g/L (250 g TiO_2 particles + 500 g water) were dispersed in deionized water by an ultrasonic treatment for 30 min. In the coating and aging processes, the temperature was controlled at 60 °C by a constant temperature bath. The procedures used were as follows.

(1) CeO_2 single layer coating: 0.25 mol/L $Ce(SO_4)_2$ or $Ce(NO_3)_3$ solution and 4.5 mol/L NaOH solution were together titrated into the TiO_2 suspension. The TiO_2 suspension was stirred vigorously and its pH was controlled at 9 by adjusting the titration rate of the NaOH solution with the titration rate of the $Ce(SO_4)_2$ or $Ce(NO_3)_3$ solution kept constant. After the titration, the suspension was aged for 2 h with stirring. Then, the coated TiO_2 particles were filtrated out, washed repeatedly, and dried at 105 °C for 24 h. The coated amounts of CeO_2 were from 0.1 to 1.0 wt % (CeO_2/TiO_2).

(2) CeO_2 + SiO_2 and CeO_2 + Al_2O_3 double layer coating: For the CeO_2 + SiO_2 double layer coating, the CeO_2 coating process was the same as the CeO_2 single layer coating, with the coating amount varied from 0.2 to 1.0 wt % (CeO_2/TiO_2). A 1.0 mol/L Na_2SiO_3 solution and 1.0 mol/L H_2SO_4 solution were together titrated into the CeO_2 coated TiO_2 suspension at a constant pH of 9, which was kept constant by adjusting the titration rate of the H_2SO_4 solution at a constant titration rate of the Na_2SiO_3 solution. The SiO_2 coating amount was fixed at 2.0 wt % (SiO_2/TiO_2). The suspension was then aged for another 2 h under stirring. For CeO_2 + Al_2O_3 double layer coating, the coating process was the same as the CeO_2 + SiO_2 double layer coating. 0.50 mol/L $Al_2(SO_4)_3$ solution and 4.5 mol/L NaOH solution were together titrated into the CeO_2 coated TiO_2 suspension at a constant pH of 5 by adjusting the titration rate of the NaOH solution at a constant titration rate of the $Al_2(SO_4)_3$ solution. The Al_2O_3 coating amount was fixed at 1.5 wt % (Al_2O_3/TiO_2).

(3) CeO_2 + SiO_2 and CeO_2 + Al_2O_3 composite coating: For the CeO_2 + SiO_2 composite coating, a mixed solution of 0.25 mol/L $Ce(SO_4)_2$ with a fixed amount of H_2SO_4, together with 1 mol/L Na_2SiO_3 solution were both together titrated into the TiO_2 suspension at constant rates. The coating amounts of CeO_2 were from 0.2 to 1.0 wt %, and the coating amount of SiO_2 was fixed at 2.0 wt % (SiO_2/TiO_2). The slurry pH was not controlled, but it stayed at about 9. After the titration, the suspension was aged for 2 h under stirring. For the CeO_2 + Al_2O_3 composite coating, the coating process was the same as the CeO_2 + SiO_2 composite coating. A mixed solution of 0.25 mol/L $Ce(SO_4)_2$ and 0.50 mol/L $Al_2(SO_4)_3$, together with 4.5 mol/L NaOH solution were both together titrated into the TiO_2 suspension at constant

dx.doi.org/10.1021/ie402539n | Ind. Eng. Chem. Res. 2014, 53, 189−197

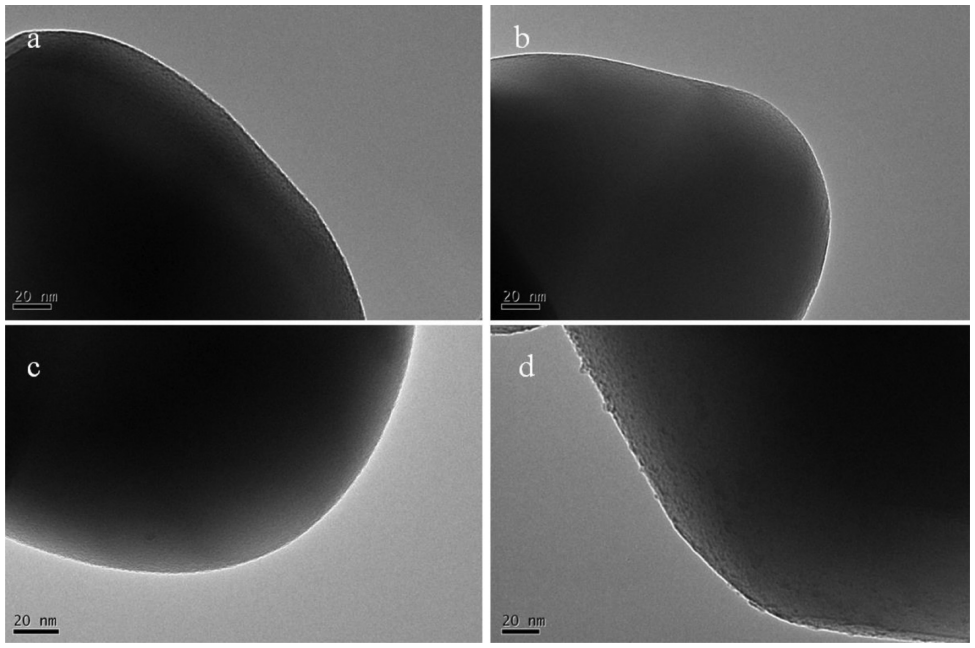

Figure 2. HRTEM images of the surface morphology of CeO_2-coated TiO_2 particles with coated amount (wt %): (a) 0.1, (b) 0.2, (c) 0.5, and (d) 1.0.

rates. The coating amount of Al_2O_3 was fixed at 1.5 wt % (Al_2O_3/TiO_2). The slurry pH was not controlled, and it decreased from about 9 to 5.

(4) SiO_2 and Al_2O_3 single layer coating: For the SiO_2 single layer coating, 2.0 wt % SiO_2 was coated at pH 9 with the same procedure as the CeO_2 single layer coating. Then, the suspension was aged for 2 h under stirring. The coated TiO_2 particles were filtrated out using a vacuum pump and then washed repeatedly. The filter cakes were dried at 105 °C for 24 h. For the Al_2O_3 single layer coating, the coating procedure was the same as the CeO_2 single layer coating. $Al_2(SO_4)_3$ solution and NaOH solution were together titrated into the TiO_2 suspension at a controlled pH of 5. The Al_2O_3 coating amount was 1.5 wt %.

2.3. Characterization. The morphology and structure of the coated TiO_2 particles were examined with a high resolution transmission electron microscope (HRTEM, JEM-2011, JEOL Co., Tokyo, Japan). Samples for HRTEM analysis were dispersed in ethanol by ultrasonic treatment for 30 min. The distribution of the coated elements on the TiO_2 particle surface was obtained by EDS mapping. X-ray photoelectron spectra (XPS, PHI Quantera SXM, ULVACPHI, Japan) was used to characterize the atomic binding energies. The coating amounts were determined with X-ray fluorescence spectroscopy (XRF, Shimadzu XRF-1800, Japan).

2.4. Photocatalytic Activity Evaluation. The photocatalytic activity of the coated TiO_2 particles was evaluated by rhodamine-B degradation. Coated or noncoated TiO_2 particles at a concentration of 4 g/L were dispersed in 4 mg/L rhodamine-B solution. The suspension was stirred vigorously for 30 min in the dark during the adsorption process, which was carried out at a constant temperature and air flow rate. Then, the suspension was irradiated with ultraviolet low pressure mercury lamps (dominant wavelength 254 nm, 32 W) for 120 min.[31] Samples of the suspension were taken every 30 min and centrifuged for 10 min. The suspension supernatant liquid was analyzed with a UV−visible spectrophotometer (TU-1901 Persee, Beijing, China). The characteristic absorbance of rhodamine-B at 554 nm was used to measure the concentration of rhodamine-B, which was inversely related to the degradation rate of rhodamine-B.

2.5. Photodegradation Kinetics of TiO_2. The photodegradation kinetics of TiO_2 particles is a classical heterogeneous catalytic reaction which follows the Langmuir adsorption model.[32−35] It has the following steps: (1) transfer of reactants from the fluid phase to the surface, (2) adsorption of the reactants, (3) reaction in the adsorbed phase, (4) desorption of the products, and (5) transfer of products into the fluid phase. The rate expression from the Langmuir−Hinshelwood kinetics is often approximated by a first-order kinetic expression when the rhodamine-B concentration is less than 10^{-3} M[7]

$$r = -\frac{dC}{dt} = \frac{k_r KC}{1 + KC} \approx k_r KC = k_{app} C \tag{14}$$

$$\ln(C/C_0) = -k_{app} t \tag{15}$$

r is the reaction rate in milligrams per liter minute, C is the concentration of rhodamine-B in milligrams per liter; t is the reaction time in minutes, k_r is the reaction rate constant in milligrams per liter minute, K is the adsorption equilibrium constant in liters per milligram, k_{app} is an apparent first-order rate constant in inverse minutes, and C_0 is the initial concentration in the solution after saturation adsorption in milligrams per liter. At 30 min intervals, the rhodamine-B concentration was measured (C_i, i = 0, 1, ..., 4). The data points gave a fitted straight line of $\ln(C/C_0)$ versus t, with a slope that is the apparent first-order rate constant. A smaller k_{app} indicates a slower degradation rate and a larger decrease in the photocatalytic activity of the TiO_2 particles.

3. RESULTS AND DISCUSSION

3.1. Coating with Cerium Oxide. The TEM images of CeO_2-coated TiO_2 particles with nominal CeO_2 coating

dx.doi.org/10.1021/ie402539n | Ind. Eng. Chem. Res. 2014, 53, 189−197

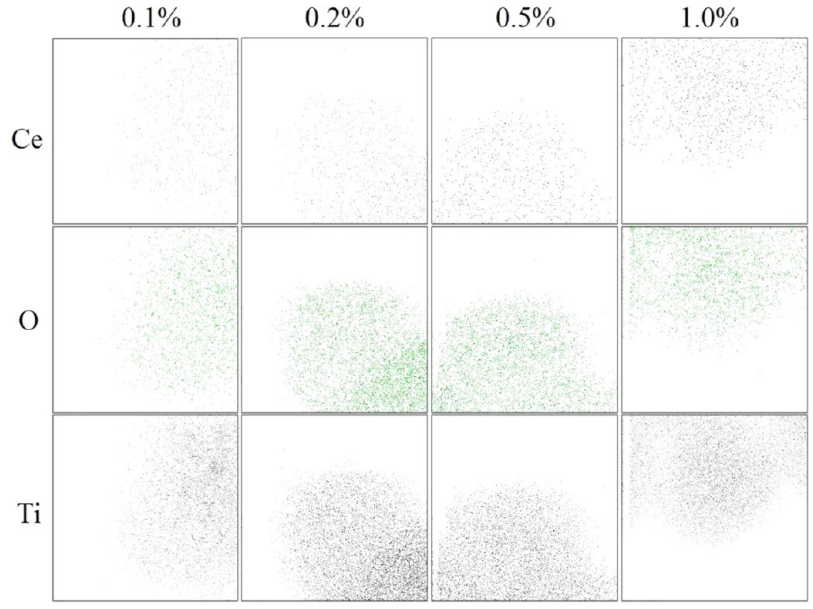

Figure 3. EDS mapping images of the surface distribution of CeO_2-coated TiO_2 particles with coated amount (wt %): (a) 0.1, (b) 0.2, (c) 0.5, and (d) 1.0.

amounts of 0.1, 0.2, 0.5, and 1.0 wt % are shown in Figure 2. There was no clearly observable continuous film with the nominal CeO_2 coating amounts of 0.1, 0.2, and 0.5 wt % in Figure 2a, b, and c. Some CeO_2 film fragments coated on the TiO_2 particle surface can be seen when the nominal CeO_2 coating amount was 1.0 wt %. The surface coatings were further characterized by EDS mapping. The results are shown in Figure 3, which showed that for all the coating amounts, the CeO_2 was uniformly distributed on the TiO_2 particle surface. The actual amounts of CeO_2 coated on the TiO_2 particle surface measured by XRF are listed in Table 1. The actual coating amounts were basically proportional to the nominal coating amounts.

Table 1. Coating Amount of Cerium Oxide on the Surface of TiO_2 Measured by XRF

nominal, wt %	measured, wt %
0.1	0.113
0.2	0.234
0.5	0.531
1.0	0.892

The photocatalytic activity of the CeO_2-coated TiO_2 particles measured by rhodamine-B degradation under ultraviolet irradiation is shown in Figure 4. When the coating amount of CeO_2 was larger than 0.2 wt %, all the CeO_2-coated TiO_2 particles gave large decreases in photocatalytic activity. The rhodamine-B conversions due to the CeO_2-coated TiO_2 were only 12−14% after 2 h ultraviolet irradiation, while the degradation conversion due to uncoated TiO_2 was nearly 66%. The apparent first-order rate constants k_{app} for rhodamine-B degradation are listed in Table 2. A lower apparent first-order rate constant indicates a larger decrease in photocatalytic activity. As shown in Table 2, the amount of decrease in photocatalytic activity due to the coated TiO_2 increased with increasing CeO_2 coating amount from 0 to 0.2 wt %, and then, further increased slowly in the range of 0.2 to 1.0 wt %. This indicated that the coating amount of 0.2 wt % was already large enough to give excellent control of

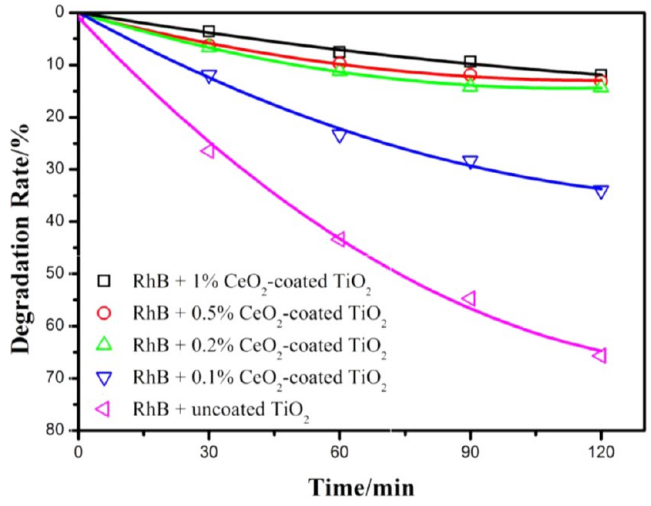

Figure 4. Degradation of rhodamine-B by CeO_2-coated TiO_2 particles with different coating amounts.

Table 2. Apparent First-Order Rate Constant k_{app} for Different Coating Amounts of Cerium Oxide

	coating, wt %	$k_{app} \times 10^3$	R^2
CeO_2	0	9.00	0.998
	0.1	3.69	0.990
	0.2	1.53	0.956
	0.5	1.35	0.962
	1.0	1.11	0.993
SiO_2	2.0	5.16	0.995
Al_2O_3	1.5	3.00	0.989

photocatalytic activity. The amount of decrease due to the TiO_2 particles coated with CeO_2 at the coating amount of 0.2 wt % was much larger than the decrease given by TiO_2 particles with a conventional film coating of 2.0 wt % SiO_2 or 1.5 wt % Al_2O_3. This means that the CeO_2 coating film had remarkably

dx.doi.org/10.1021/ie402539n | Ind. Eng. Chem. Res. 2014, 53, 189−197

controlled the photocatalytic activity even when present at just a tiny coating amount.

3.2. Combination Coating of Cerium Oxide and Silicon Oxide. In order to investigate the interaction between cerium oxide and other oxides, combination coatings of cerium oxide with silicon or aluminum oxide were made using coprecipitation to prepare these coatings. Two types of coating structures, double layer coating and composite coating, were used.

For the combination coating of cerium oxide and silicon oxide, the amounts of cerium oxide were 0.2 to 1.0 wt %, and the amount of silicon was fixed at 2.0 wt %. The HRTEM images of the particles with the CeO_2 + SiO_2 double layer coating and CeO_2 + SiO_2 composite coating are shown in Figure 5. Continuous and dense films of about 3 nm thickness

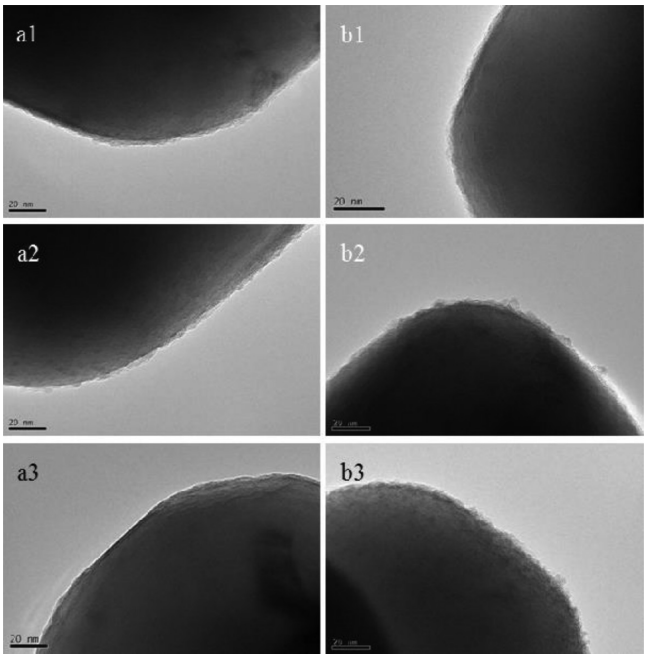

Figure 5. HRTEM images of the surface morphology of CeO_2 + SiO_2 coated TiO_2 particles at different coating amount of CeO_2 and 2.0 wt % SiO_2. Composite coating CeO_2, wt %, (a1) 0.2, (a2) 0.5, and (a3) 1.0; double layer coating CeO_2, wt %, (b1) 0.2, (b2) 0.5, and (b3) 1.0.

were coated on the surface of the 300 nm TiO_2 particles. The coat compositions of the cerium and silicon oxides measured by XRF are listed in Table 3. The data showed that the actual cerium and silicon oxide amounts coated on the TiO_2 particle surface were basically proportional to the nominal coating amounts.

The apparent first-order rate constants k_{app} are listed in Table 4. The k_{app} values of the TiO_2 particles with the CeO_2 + SiO_2 double layer coating were much higher than those of the TiO_2 particles with the pure CeO_2 coating, which was unexpected because a silicon dioxide coating also decreases the photocatalytic activity of TiO_2 particles. Meanwhile, TiO_2 particles with the CeO_2+SiO_2 composite coating had the same photocatalytic activity decrease as the single cerium oxide coating, while the k_{app} value was a little higher than those of the particles with the pure cerium oxide coating. This showed that at the same coating amount of cerium oxide, a dense film coating of cerium oxide (pure cerium oxide coating) can give a larger decrease in photocatalytic activity, but a low density film

Table 3. Apparent First-Order Rate Constant k_{app} for Different Coating Amounts of Cerium and Silicon or Aluminum Oxide

	SiO_2 2.0 wt %			Al_2O_3 1.5 wt %		
	CeO_2, wt %	$k_{app} \times 10^3$	R^2	CeO_2, wt %	$k_{app} \times 10^3$	R^2
composite coating	0.2	1.57	0.999	0.2	2.38	0.964
	0.5	1.42	0.994	0.5	1.34	0.996
	1.0	1.32	0.992	1.0	1.87	0.973
double-layer coating	0.2	2.51	0.997	0.2	1.80	0.959
	0.5	1.84	0.995	0.5	1.30	0.949
	1.0	1.77	0.993	1.0	2.06	0.979

cerium oxide coating (which was diluted by silicon oxide) obtained by coprecipitation with silicon oxide gave a smaller decrease in photocatalytic activity.

In summary, TiO_2 particles coated with pure cerium oxide gave the largest decrease in photocatalytic activity, with the composite coating of CeO_2 + SiO_2 (cerium oxide coating of low density) giving a smaller amount of decrease and the double layer coating of CeO_2 + SiO_2 giving the least decrease in photocatalytic activity. For the double layer coating and composite coating, the amount of decrease in photocatalytic activity increased with the nominal coating amount of cerium oxide.

3.3. Combination Coating of Cerium Oxide and Aluminum Oxide. For the combination coating of cerium oxide and aluminum oxide, the coating amounts of cerium oxide were from 0.2 to 1.0 wt %, and the amount of aluminum was fixed at 1.5 wt %. The HRTEM images of the particles with the CeO_2 + Al_2O_3 double layer coating and CeO_2 + Al_2O_3 composite coating are shown in Figure 6. Continuous and dense films of about 3 nm thickness were coated on the surface of the 300 nm particles.

The values of the fitted k_{app} for the CeO_2 + Al_2O_3 coated TiO_2 particles are listed in Table 3. These values showed that the combination coating of cerium oxide and aluminum oxide gave smaller decreases in photocatalytic activity as compared with the pure cerium oxide coating, which was again unexpected since an aluminum oxide coating also decreased the photocatalytic activity of TiO_2 particles. The CeO_2 + Al_2O_3 double layer coated particles gave a larger decrease in photocatalytic activity than the CeO_2 + Al_2O_3 composite coated particles. This probably was a result of the pH environment used in the composite coating process. In our previous experiments, it was found that TiO_2 coated with cerium oxide in a basic environment gave a larger decrease in photocatalytic activity than those coated in an acidic environment. For the double layer coating process, the slurry was kept constant at pH 9 for 2 h, which provided an appropriate environment and enough time for the deposition of cerium oxide in a basic environment. For the composite coating, however, the slurry pH decreased from 9 to 5 and it was aged at pH 5 for 2 h, which led to a decrease in photoelectron−hole capture ability.

The coated amounts of cerium and aluminum oxides on the surface were measured by XRF. The results are shown in Table 4. The comparison of the coated amounts of cerium oxide in Tables 1 and 4 showed that both the pure cerium film and the film with a low density of cerium (diluted by aluminum oxide) have the same coating amount of cerium. However, the kinetic parameters showed clearly that TiO_2 coated with pure cerium

dx.doi.org/10.1021/ie402539n | Ind. Eng. Chem. Res. 2014, 53, 189−197

Table 4. Coating Amounts of Cerium and Silicon or Aluminum Oxide on the Surface of TiO_2 Measured by XRF[a]

	Ce-nominal, wt %	Ce-measured, wt %	Si-measured, wt %	Ce-nominal, wt %	Ce-measured, wt %	Al-measured, wt %
composite coating	0.2	0.217	2.042	0.2	0.350	1.460
	0.5	0.477	1.803	0.5	0.481	1.377
	1.0	1.067	1.782	1.0	0.854	1.451
double-layer coating	0.2	0.206	2.078	0.2	0.338	1.470
	0.5	0.475	1.805	0.5	0.555	1.389
	1.0	1.085	1.870	1.0	0.863	1.379

[a]Nominal amount: SiO_2 2.0 wt % or Al_2O_3 1.5 wt %.

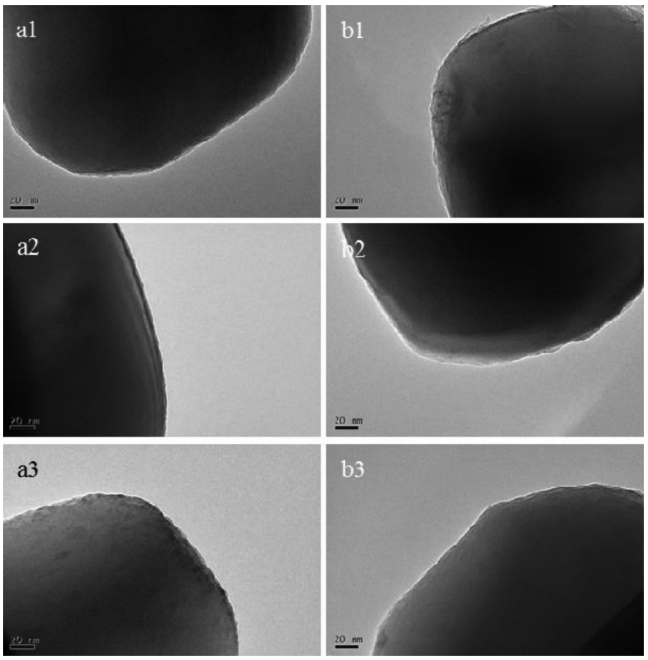

Figure 6. HRTEM images of the surface morphology of CeO_2 + Al_2O_3 coated TiO_2 particles at different coating amount of CeO_2 and 1.5 wt % Al_2O_3. Composite coating CeO_2, wt %, (a1) 0.2, (a2) 0.5, and (a3) 1.0; double layer coating CeO_2, wt %, (b1) 0.2, (b2) 0.5, and (b3) 1.0.

gave a much larger decrease in photocatalytic activity than did TiO_2 coated with the cerium coating of low density. Therefore, for a large decrease in the photocatalytic activity of TiO_2, it is essential to deposit a film coat with a high density of cerium oxide, and not a thicker coating of cerium oxide that was diluted with some other oxide.

3.4. Cerium Oxide Coating with Different Valence States. The effects of cerium oxide coatings with the cerium in different valence states on the decrease of the photocatalytic activity of TiO_2 particles were investigated. $Ce(NO_3)_3{\cdot}6H_2O$ and $Ce(SO_4)_2{\cdot}4H_2O$ were used as the coating reagents. HRTEM was used to examine the coated film of Ce(III) oxide. Similar to the Ce(IV) oxide coating, there was no observable continuous film for the coating amounts of 0.2 and 0.5 wt %. EDS mapping showed that all the different coating amounts of Ce(III) oxide gave coatings with Ce uniformly distributed on the TiO_2 particle surface. The ultraviolet irradiation experiment showed that the TiO_2 particles coated with Ce(III) oxide gave the same amount of decrease in photocatalytic activity as did the TiO_2 particles coated with Ce(IV) oxide. The k_{app} values for TiO_2 particles with the Ce(III) oxide coating were a little higher than those for the particles with the Ce(IV) oxide coating, which is shown in Table 5.

Table 5. Apparent First-Order Rate Constant k_{app} for Different Valence States of the Cerium Oxide

	Ce, wt %	$k_{app} \times 10^3$	R^2
Ce(III)	0.2	1.30	0.988
	0.5	1.04	0.998
	1.0	0.91	0.977
Ce(IV)	0.2	1.53	0.956
	0.5	1.35	0.962
	1.0	1.11	0.993

To characterize the valence state of the cerium oxide coated on the surface of the TiO_2 particles, the atomic binding energies before and after ultraviolet irradiation were measured by XPS. Figure 7 shows the O1s XPS spectra. The peak at 530.3 and 529.6 eV are the characteristic peaks of Ce(III)−O and Ce(IV)−O.[36]

For Ce(III) oxide, the O1s peak was at 530.2 eV before ultraviolet irradiation. This indicated that the cerium oxide coated on the TiO_2 particle surface was Ce(III) when the coating reagent was $Ce(NO_3)_3{\cdot}6H_2O$. After ultraviolet irradiation, the characteristic peak was shifted from 530.2 to 529.7 eV, which is the characteristic peak of Ce(IV)−O. This indicated that oxidation occurred during the ultraviolet irradiation, that is, Ce(III)−O had captured holes to form Ce(IV)−O.

The O1s peak for Ce(IV) oxide was at 529.6 eV before ultraviolet irradiation, which showed that the cerium oxide coated on the surface was Ce(IV)−O when the coating reagent was $Ce(SO_4)_2{\cdot}4H_2O$. After ultraviolet irradiation, the O1s spectrum for Ce(IV)−O was split into two peaks at 530.4 and 529.6 eV. This indicated that some Ce(IV)−O was transformed into Ce(III)−O after ultraviolet irradiation to give a mixture comprising Ce(III)−O and Ce(IV)−O on the surface of the TiO_2 particles.

The difference in the O1s spectra can explain why the k_{app} values for the Ce(III) oxide coated TiO_2 were a little higher than those for the Ce(IV) oxide coated TiO_2. Cerium has the atomic structure $[Xe]4f^15d^16s^2$, and the 4f electron subshell tends to be empty to form stable structure, that is, Ce(IV) exist in a stable structure when it is in an electronic configuration where the 4f electron orbital is empty ($4f^0$).[37] The Ce(III) oxide coating tends to capture holes, so all Ce(III) cations were transformed into stable Ce(IV), as shown in Figure 7a, which gave a larger decrease in photocatalytic activity. The Ce(IV) oxide coating, however, has a little lower ability to capture electrons, so only part of the Ce(IV) cations were transformed into Ce(III), as shown in Figure 7b, which resulted in a smaller decrease in photocatalytic activity than that given by the Ce(III) oxide coating.

3.5. Mechanism of How the Cerium Oxide Coating Decreased the Photocatalytic Activity. EDS mapping and

dx.doi.org/10.1021/ie402539n | Ind. Eng. Chem. Res. 2014, 53, 189−197

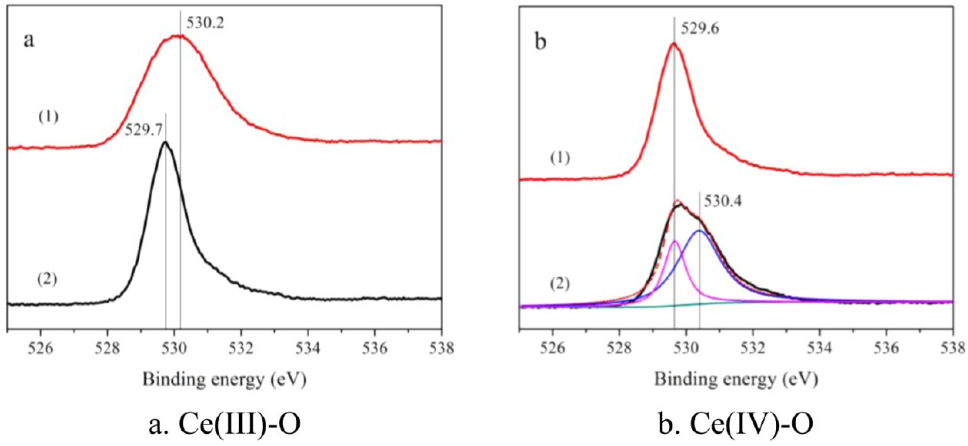

Figure 7. O1s spectra of TiO_2 coated with Ce(III)−O and Ce(IV)−O (1) before ultraviolet irradiation and (2) after 2 h ultraviolet irradiation.

XRF analysis confirmed that the cerium oxide of the different coating amounts were all uniformly distributed on the TiO_2 particle surface, even when the coating amount was small. It was estimated that a continuous and dense film of one molecular layer of CeO_2 coated on the particle surface would require a coating amount of cerium oxide of 1.84 wt %, which was much higher than the coating amounts used in the experiments. The calculation is as follows. The average diameter of the TiO_2 particles is 300 nm, and the density of rutile titanium dioxide is 4200 kg/m^3. For a single TiO_2 particle,

$$S_{TiO_2} = \pi d_{TiO_2}{}^2 = 2.826 \times 10^{-13}\ m^2 \quad (16)$$

$$V_{TiO_2} = \frac{1}{6}\pi d_{TiO_2}{}^3 = 1.413 \times 10^{-20}\ m^3 \quad (17)$$

$$m_{TiO_2} = \rho_{TiO_2} V_{TiO_2} = 5.918 \times 10^{-17}\ kg \quad (18)$$

The cell length of CeO_2 is a_{CeO_2} = 0.541 nm[38] and the density of CeO_2 is 7130 kg/m^3. For one molecular layer of CeO_2 coated on the surface, this gives

$$V_{CeO_2} = S_{TiO_2} a_{CeO_2} = 1.529 \times 10^{-22}\ m^3 \quad (19)$$

$$m_{CeO_2} = \rho_{CeO_2} V_{CeO_2} = 1.090 \times 10^{-18}\ kg \quad (20)$$

So the mass fraction of CeO_2 would be

$$w_{CeO_2} = \frac{m_{CeO_2}}{m_{TiO_2}} \times 100\% = 1.84\% \quad (21)$$

This indicated that the cerium was distributed on the particle surface not as a continuous film but as uniformly distributed spotty coatings. However, the cerium coating even as a spotty coating can effectively capture electrons and holes. It was inferred that it was not necessary to have a continuous and dense film like the conventional coatings of silicon or aluminum oxide used to prevent the electrons and holes from escaping from the TiO_2. The excellent control of photocatalytic activity by the coated TiO_2 particles was attributed to the cerium oxide coating acting as an electron−hole trap.

Cerium has the atomic structure $[Xe]4f^15d^16s^2$, with unpaired 4f orbital electrons which can capture electrons and holes. The valence change between Ce(III) and Ce(IV), as discussed in section 3.4, increased the ability to capture the electrons and holes produced by ultraviolet irradiation. The cerium coated on the surface provide indirect recombination sites for the electrons and holes to prevent their transport to the surface of the TiO_2 particles, where they otherwise would produce highly active free radicals.

Meanwhile, since Ce(IV) has a stronger oxidability than Ti(IV), it captures electrons more easily than Ti(IV), and this reduces the formation of Ti^{3+} on the particle surface (see eq 9). For TiO_2 particles, a high concentration of Ti^{3+} on the surface leads to a high photocatalytic activity. The decrease in the concentration of Ti^{3+} would result in the decreased photocatalytic activity of the cerium oxide coated TiO_2.

For the combination coating of cerium oxide with silicon or aluminum oxide, the silicon or aluminum oxide probably serves as a filler which lowers the density of cerium oxide in the film. This leads to decreased electron−hole capture ability, as compared with cerium oxide with a high density that can capture electrons and holes rapidly and effectively. Thus, both the amount and density of the cerium oxide play important roles in giving more decrease in the photocatalytic activity of TiO_2 particles.

The interface between cerium oxide and silicon or aluminum oxide attenuates some decrease in photocatalytic activity. At the interface between CeO_2 and SiO_2 or Al_2O_3, a new hybridized orbital can form, which can prevent the recombination of electrons and holes. This led to the attenuation of the decrease in the photocatalytic activity of TiO_2 coated with a CeO_2 + SiO_2 or CeO_2 + Al_2O_3 double layer coating.

Therefore, it was inferred that the electronic structure of cerium was the key factor that gave a large decrease in photocatalytic activity. The detailed mechanism still needs further study.

4. CONCLUSIONS

A cerium oxide coating gave a large decrease in the photocatalytic activity of TiO_2 particles even when present as a spotty (noncontinuous) coating on the surface and even with a tiny coating amount of 0.2 wt %. The combination coatings comprising cerium oxide and silicon or aluminum oxide gave smaller decreases in photocatalytic activity as compared to that obtained with the pure cerium oxide coating, even though either a silicon or aluminum oxide coating by itself also gave a decrease in the photocatalytic activity of TiO_2 particles. TiO_2 particles coated with Ce(III) oxide gave a slightly larger decrease in photocatalytic activity than a Ce(IV) oxide coat. Cerium oxide can effectively capture photogenerated electrons

dx.doi.org/10.1021/ie402539n | Ind. Eng. Chem. Res. 2014, 53, 189−197

and holes, which does not allow the electrons and holes to diffuse to the surface of TiO_2, which leads to the significant decrease in photocatalytic activity.

AUTHOR INFORMATION

Corresponding Author

*Tel.: +86-10-62788993. Fax: +86-10-62772051. E-mail: wangtj@tsinghua.edu.cn.

Notes

The authors declare no competing financial interest.

ACKNOWLEDGMENTS

The authors wish to express their appreciation of the financial support of this study by the National Natural Science Foundation of China (NSFC No. 21176134).

REFERENCES

(1) Taylor, M. L.; Morris, G. E.; Smart, R. S. Influence of aluminum doping on titania pigment structural and dispersion properties. *J. Colloid Interface Sci.* **2003**, *262*, 81−88.

(2) Sidky, P. S.; Hocking, M. G. Review of inorganic coatings and coating processes for reducing wear and corrosion. *Br. Corros J.* **1999**, *34*, 171−183.

(3) Hakim, L. F.; King, D. M.; Zhou, Y.; Gump, C. J.; George, S. M.; Weimer, A. W. Nanoparticle coating for advanced optical, mechanical and rheological properties. *Adv. Funct. Mater.* **2007**, *17*, 3175−3181.

(4) Katoh, R.; Murai, M.; Furube, A. Electron-hole recombination in the bulk of a rutile TiO_2 single crystal studied by sub-nanosecond transient absorption spectroscopy. *Chem. Phys. Lett.* **2008**, *461*, 238−241.

(5) Coronado, J. M.; Maira, A. J.; Martinez-Arias, A.; Conesa, J. C.; Soria, J. EPR study of the radicals formed upon UV irradiation of ceria-based photocatalysts. *J. Photochem. Photobiol. A: Chem.* **2002**, *150*, 213−221.

(6) Scotti, R.; Bellobono, I. R.; Canevali, C.; Cannas, C.; Catti, M.; D'Arienzo, M.; Musinu, A.; Polizzi, S.; Sommariva, M.; Testino, A.; Morazzoni, F. Sol-gel pure and mixed-phase titanium dioxide for photocatalytic purposes: Relations between phase composition, catalytic activity, and charge-trapped sites. *Chem. Mater.* **2008**, *20*, 4051−4061.

(7) Li, Y.; Sun, S.; Ma, M.; Ouyang, Y.; Yan, W. Kinetic study and model of the photocatalytic degradation of rhodamine B (RhB) by a TiO_2-coated activated carbon catalyst: Effects of initial RhB content, light intensity and TiO_2 content in the catalyst. *Chem. Eng. J.* **2008**, *142*, 147−155.

(8) de Lara-Castells, M. P.; Krause, J. L. Theoretical study of the interaction of molecular oxygen with a reduced TiO_2 surface. *Chem. Phys. Lett.* **2002**, *354*, 483−490.

(9) Wei, B. X.; Wang, T. J.; Zhao, L.; Chen, L.; Jin, Y. Photocatalytic reaction process on titania particle surface. *Pet. Technol.* **2012**, *41*, 219−223.

(10) Green, J.; Carter, E.; Murphy, D. M. Interaction of molecular oxygen vacancies on reduced TiO_2:Site specific blocking by probe molecules. *Chem. Phys. Lett.* **2009**, *477*, 340−344.

(11) Berger, T.; Diwald, O.; Knozinger, E.; Napoli, F.; Chiesa, M.; Giamello, E. Hydrogen activation at TiO_2 anatase nanocrystals. *Chem. Phys.* **2007**, *339*, 138−145.

(12) Sirisuk, A.; Klansorn, E.; Praserthdam, P. Effects of reaction medium and crystallite size on Ti^{3+} surface defects in titanium dioxide nanoparticles prepared by solvothermal method. *Catal. Commun.* **2008**, *9*, 1810−1814.

(13) Komaguchi, K.; Maruoka, T.; Nakano, H.; Imae, I.; Ooyama, Y.; Harima, Y. ESR study on the reversible electron from O_2^{2-} to Ti^{4+} on TiO_2 nanoparticles induced by visible-light illumination. *J. Phys. Chem. C.* **2009**, *113*, 1160−1163.

(14) Komaguchi, K.; Nakano, H.; Araki, A.; Harima, Y. Photoinduced electron transfer from anatase to rutile in partially reduced TiO_2 (P-25) nanoparticles: An ESR study. *Chem. Phys. Lett.* **2006**, *428*, 338−342.

(15) Nakaoka, Y.; Nosaka, Y. ESR inverstigation into the effects of heat treatment and crystal structure on radicals produced over irradiated TiO_2 powder. *J. Photochem. Photobiol. A.* **1997**, *110*, 299−305.

(16) Howe, R. F.; Gratzel, M. Electron-paramagnetic-res observation of trapped electrons in colloidal TiO_2. *J. Phys. Chem.* **1985**, *89*, 4495−4499.

(17) Park, D. R.; Zhang, J. L.; Ikeue, K.; Yamashitab, H.; Anpob, M. Photocatalytic oxidation of ethylene to CO_2 and H_2O on ultrafine powdered TiO_2 photocatalysts in the presence of O_2 and H_2O. *J. Catal.* **1999**, *185*, 114−119.

(18) Suriye, K.; Praserthdam, P.; Jongsomjit, B. Control of Ti^{3+} surface defect on TiO_2 nanocrystal using various calcination atmospheres as the first step for surface defect creation and its application in photocatalysis. *Appl. Surf. Sci.* **2007**, *253*, 3849−3855.

(19) Carter, E.; Carley, A. F.; Murphy, D. M. Evidence for O_2^- radical stabilization at surface oxygen vacancies on polycrystalline TiO_2. *J. Phys. Chem.* **2007**, *111*, 10630−10638.

(20) Zhao, J. C.; Wu, T. X.; Wu, K. Q.; Oikawa, K.; Hidaka, H.; Serpone, N. Photoassisted degradation of dye pollutants. 3. Degradation of the cationic dye rhodamine B in aqueous anionic surfactant/TiO_2 dispersions under visible light irradiation: Evidence for the need of substrate adsorption on TiO_2 particles. *Environ. Sci. Technol.* **1998**, *32*, 2394−2400.

(21) Chen, S.; Zhang, S.; Zhao, W.; Liu, W. Study on the photocatalytic activity of TiN/TiO_2 nanoparticle formed by ball milling. *J. Nanopart. Res.* **2009**, *11*, 931−938.

(22) Wu, T. X.; Liu, G. M.; Zhao, J. C.; Hidaka, H.; Serpone, N. Photoassisted degradation of dye pollutants. V. Self-photosensitized oxidative transformation of Rhodamine B under visible light irradiation in aqueous TiO_2 dispersions. *J. Phys. Chem. B.* **1998**, *102*, 5845−5851.

(23) Zhang, Y.; Yin, H.; Wang, A.; Liu, C.; Yu, L.; Jiang, T.; Hang, Y. Evolution of zirconia coating layer on rutile TiO_2 surface and the pigmentary property. *J. Phys. Chem. Solids.* **2010**, *71*, 1458−1466.

(24) Wu, H. X.; Wang, T. J.; Jin, Y. Film-coating process of hydrated alumina on TiO_2 particles. *Ind. Eng. Chem. Res.* **2006**, *45*, 1337−1342.

(25) Ryan, J. N.; Elimelech, M.; Baeseman, J. L.; Magelky, R. D. Silica-coated titania and zirconia colloids for subsurface transport field experiments. *Environ. Sci. Technol.* **2000**, *34*, 2000−2005.

(26) Zhou, H.; Li, H.; Wei, K. *Titanium dioxide paint comprises rutile type or anatase type titanium dioxide particle composed of zirconia, amorphous silica and hydrated alumina coating*. China Patent, 2006.

(27) Idei, T. *Particulate titanium dioxide composition used for coating material, is obtained by coating titanium-dioxide surface with silicon-containing hydroxide, and depositing zirconium- containing hydroxide and aluminum-containing hydroxide*. Japan Patent, 2008.

(28) Wei, B. X.; Zhao, L.; Wang, T. J.; Gao, H.; Wu, H. X.; Jin, Y. Weather durability of TiO_2 particles coated with several transition metal oxides and its measurement by rhodamine-B degradation. *Adv. Powder Technol.* **2013**, *24*, 708−713.

(29) Jacobson, H. W. *Titanium dioxide pigment bearing a coating with cerium cations and sulfate-, phosphate-, or silicate anions*. EP Patent 0129960, 1987.

(30) Baldwin, R. A.; Brand, J. R.; Brownbridge, T. I. *Durable pigmentary titanium dioxide and methods of producing the same*. US Patent 005730796A, 1998.

(31) Zhao, L.; Gao, H.; Wei, B. X.; Wang, T. J.; Jin, Y. Evaluation of photocatalytic activity of pigmentary titania. *CIESC J.* **2013**, *64*, 2453−2461.

(32) Bhatkhande, D. S.; Pangarkar, V. G.; Beenackers, A. A. Photocatalytic degradation for environmental applications - a review. *J. Chem. Technol. Biotechnol.* **2002**, *77*, 102−116.

(33) Fox, M. A.; Dulay, M. T. Heterogeneous photocatalysis. *Chem. Rev.* **1993**, *93*, 341−357.

(34) Herrmann, J. M. Heterogeneous photocatalysis: fundamentals and applications to the removal of various types of aqueous pollutants. *Catal. Today* **1999**, *53*, 115−129.

(35) Sauer, T.; Neto, G. C.; Jose, H. J.; Moreira, R. Kinetics of photocatalytic degradation of reactive dyes in a TiO_2 slurry reactor. *J. Photochem. Photobiol. A: Chem.* **2002**, *149*, 147−154.
(36) Praline, G.; Koel, B. E.; Hance, R. L.; Lee, H. I.; White, J. M. X-ray photoelectron study of the reaction of oxygen with cerium. *J. Electron Spectrosc.* **1980**, *21*, 17−30.
(37) Chen, R. S.; Huang, M. J.; Du, D. C.; Yuan, W. Q. *Inorganic and Analytical Chemistry*; Advanced Education Press: Beijing, 1998.
(38) Jiang, X. Y.; Lu, G. L.; Zhou, R. X.; Mao, J. X.; Chen, Y.; Zheng, X. M. Studies of pore structure, temperature-programmed reduction performance, and micro-structure of CuO/CeO_2 catalysts. *Appl. Surf. Sci.* **2001**, *173*, 208−220.